# Supporting Information for «Impact of Metal and Active Site Configurations in Hydrogenation Reactions with N-Doped Graphene Single Atom Catalysts»

Aurore E. F. Denjean, David Balcells*, Ainara Nova*

# Contents

**Structures** ..... 2
**Metal moving out of the plane** ..... 6
**Triple-ζ versus double- ζ basis sets** ..... 6
**Hydrogenation without metals** ..... 7
**NEDA Analysis** ..... 7
**Hydrogens natural charge** ..... 9
**Surface (M, Ns, Cs) natural charge change upon hydrogenation** ..... 9
**Natural metal charge** ..... 10
**Pristine structure and spin state influence** ..... 11
**Pristine to hydrogenated species: spin crossover** ..... 12

# Structures

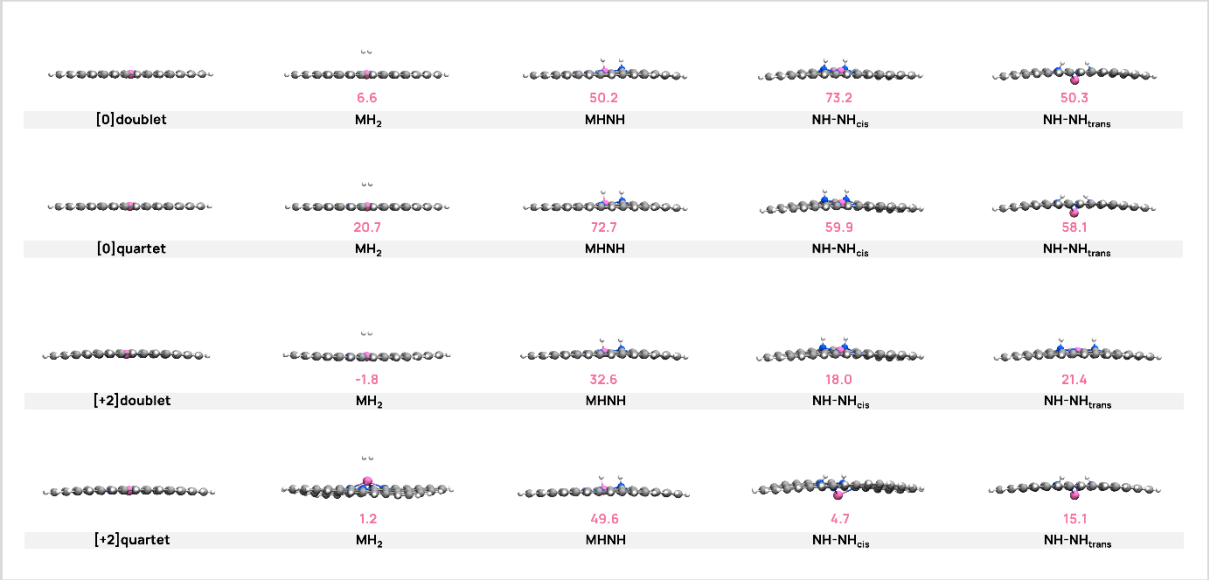


***Figure S1.*** *Optimized structures of Py Co complexes before and after $H_2$ addition, with corresponding ΔG values for the hydrogenation reaction (kcal·mol⁻¹).*

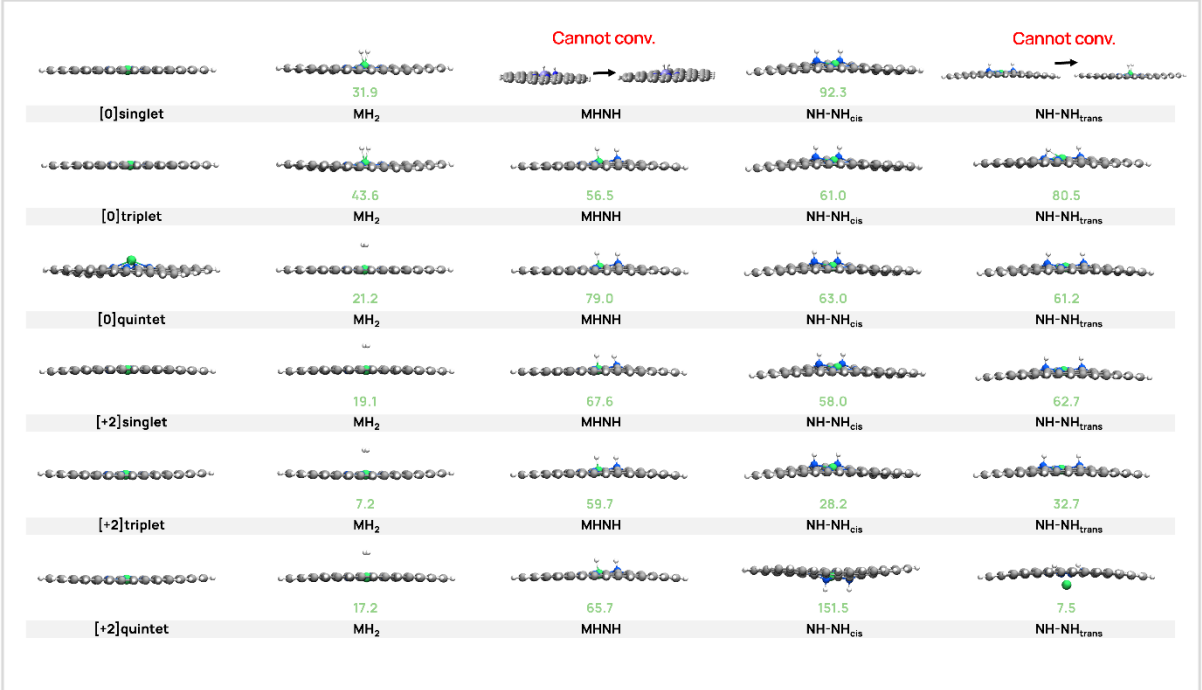


***Figure S2.*** *Optimized structures of Py Fe complexes before and after $H_2$ addition, with corresponding ΔG values for the hydrogenation reaction (kcal·mol⁻¹).*

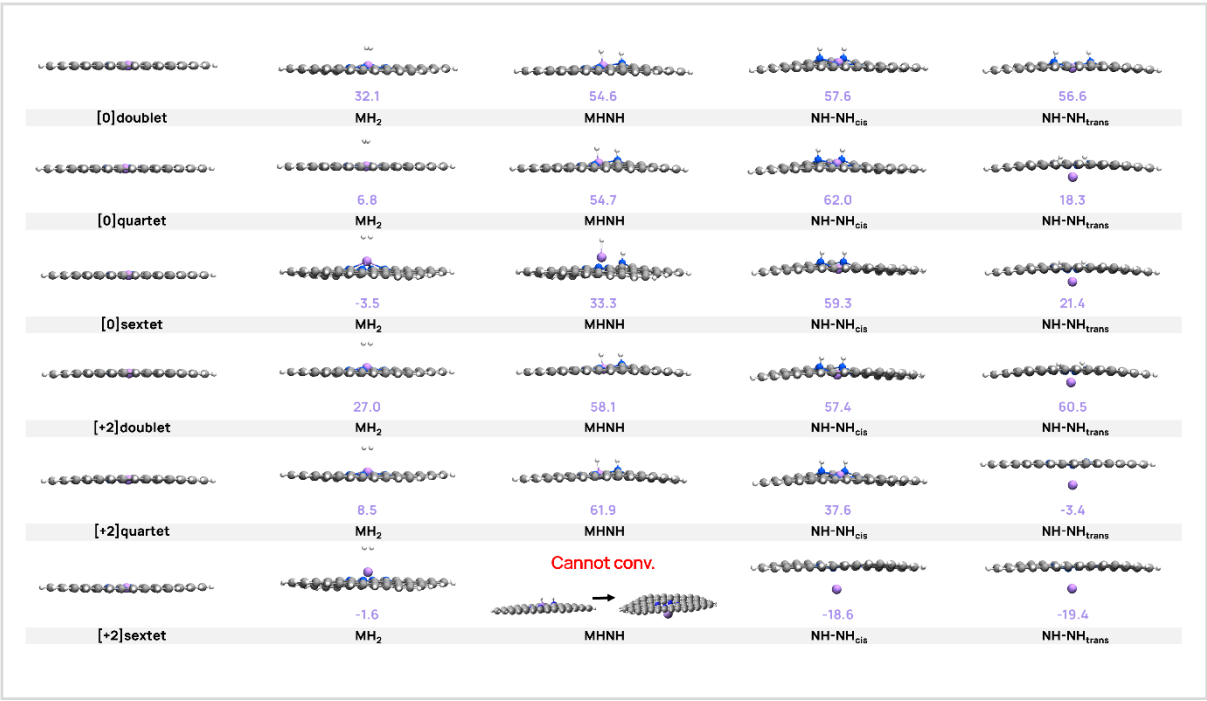


***Figure S3.*** *Optimized structures of Py Mn complexes before and after $H_2$ addition, with corresponding ΔG values for the hydrogenation reaction (kcal·mol$^{-1}$).*

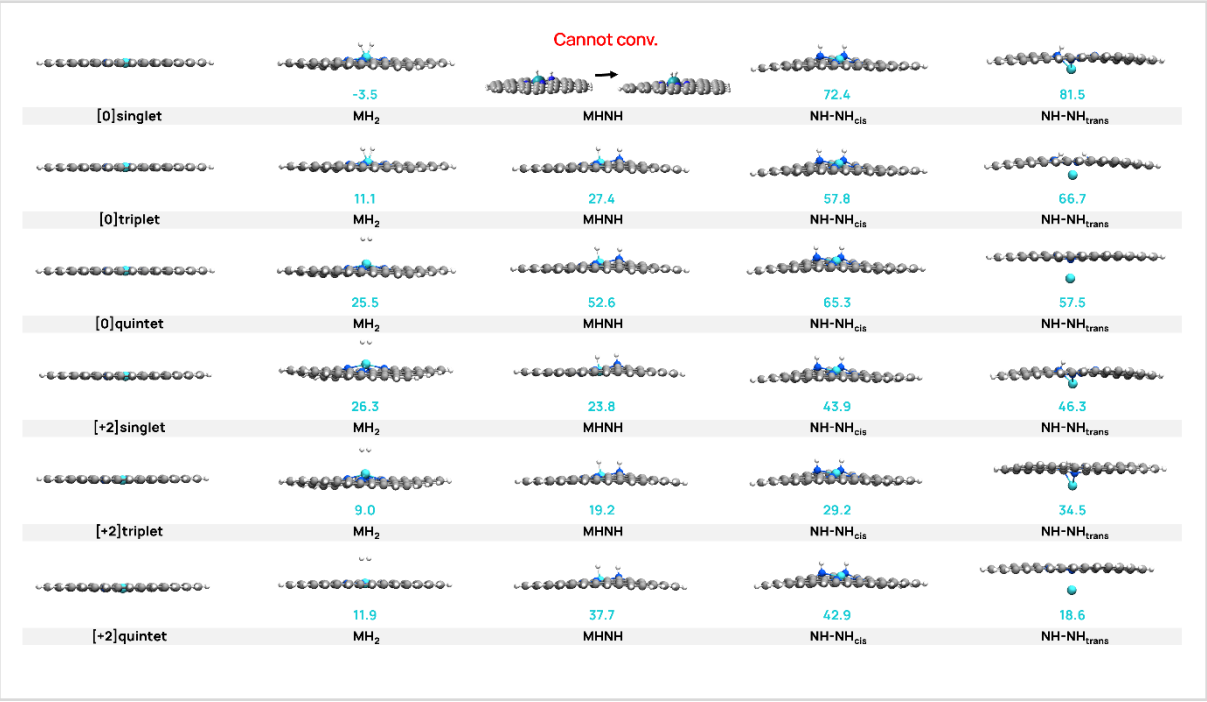


***Figure S4.*** *Optimized structures of Py Ru complexes before and after $H_2$ addition, with ΔG values for the hydrogenation reaction (kcal·mol$^{-1}$).*

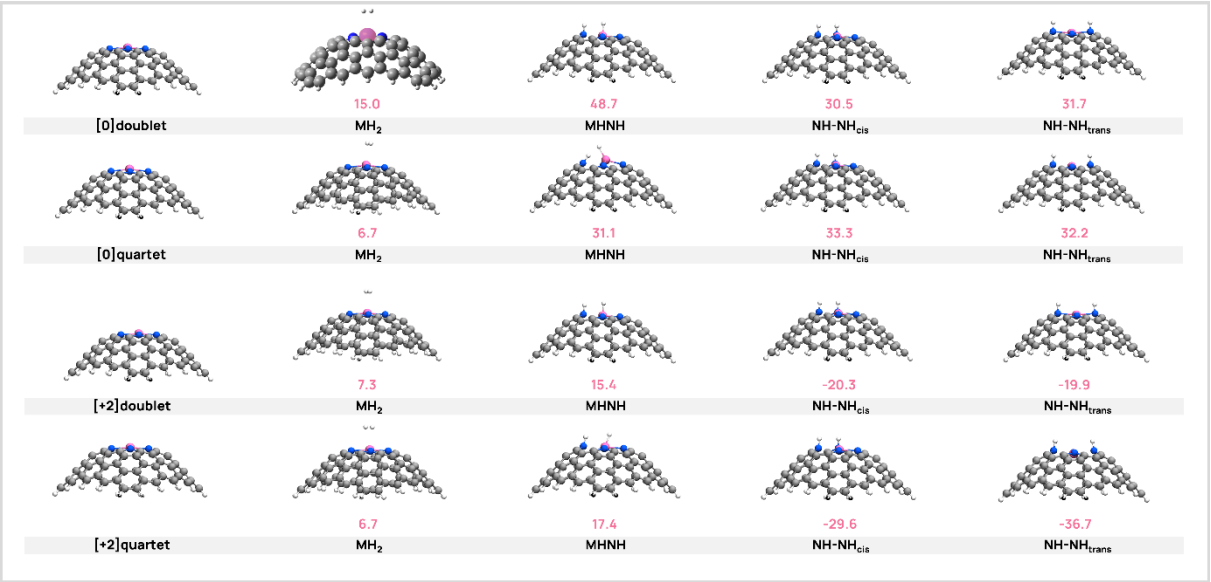


***Figure S5.*** *Optimized structures of Pyrr Co complexes before and after $H_2$ addition, with corresponding ΔG values for the hydrogenation reaction (kcal·mol⁻¹).*

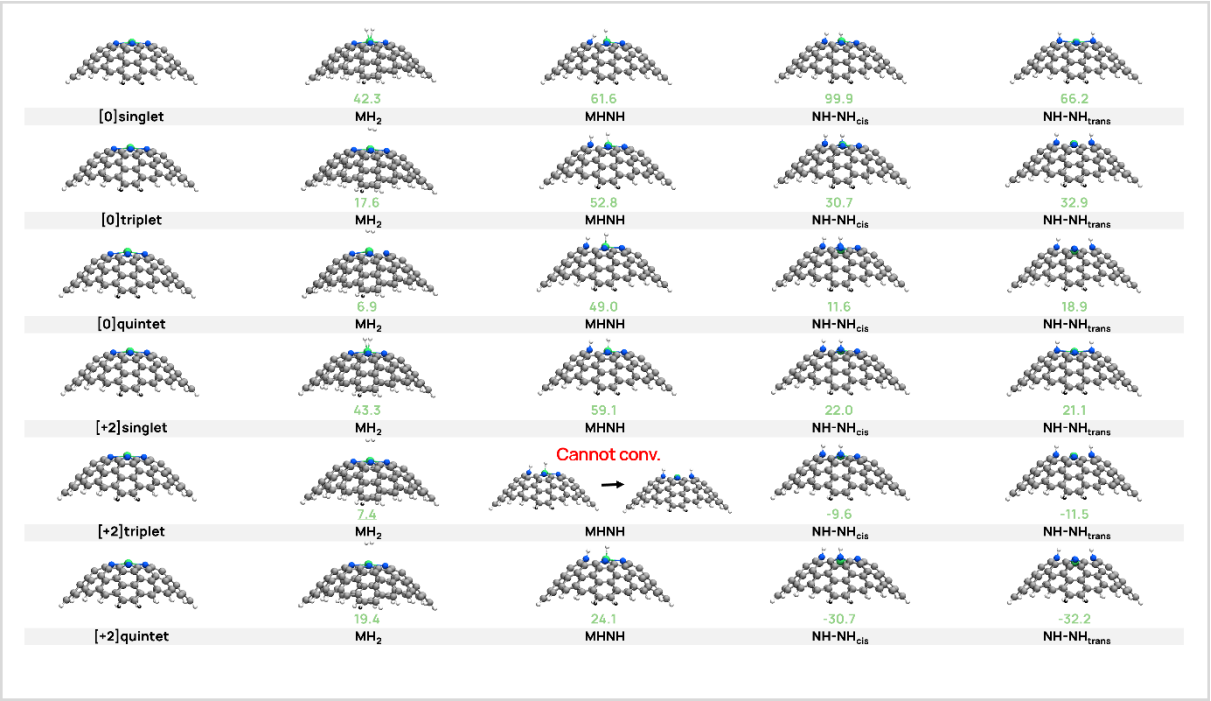


***Figure S6.*** *Optimized structures of Pyrr Fe complexes before and after $H_2$ addition, with corresponding ΔG values for the hydrogenation reaction (kcal·mol⁻¹).*

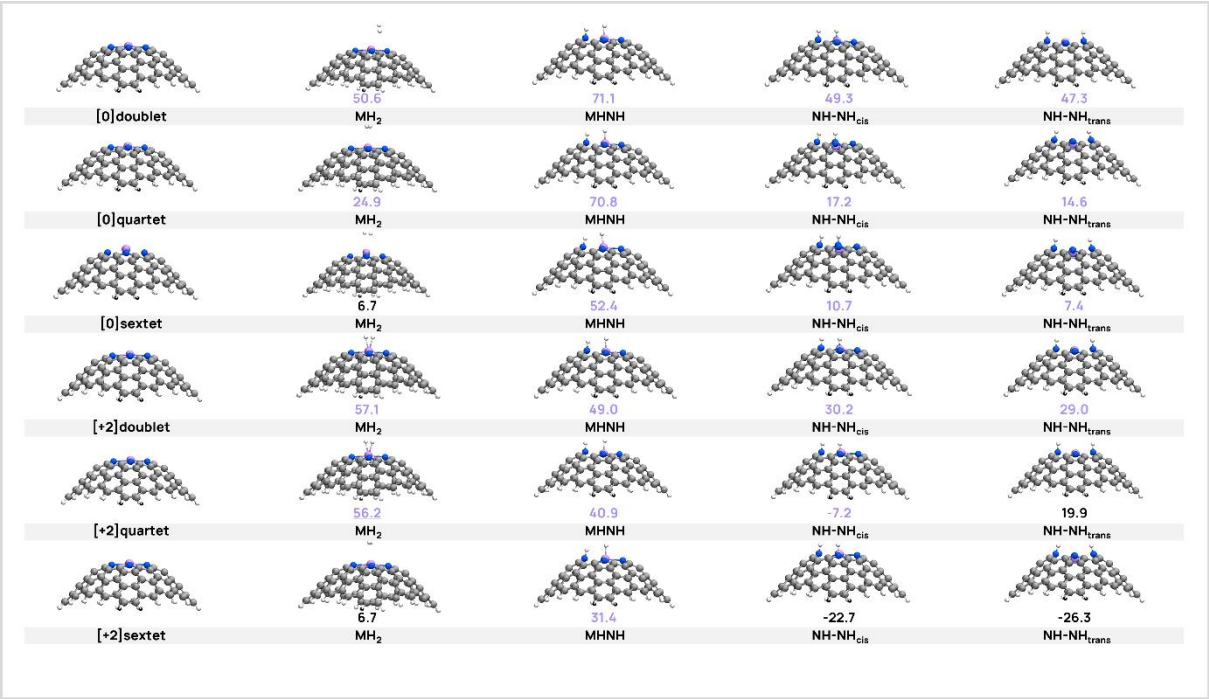


***Figure S7.*** *Optimized structures of Pyrr Mn complexes before and after $H_2$ addition, with corresponding ΔG values for the hydrogenation reaction (kcal·mol⁻¹).*

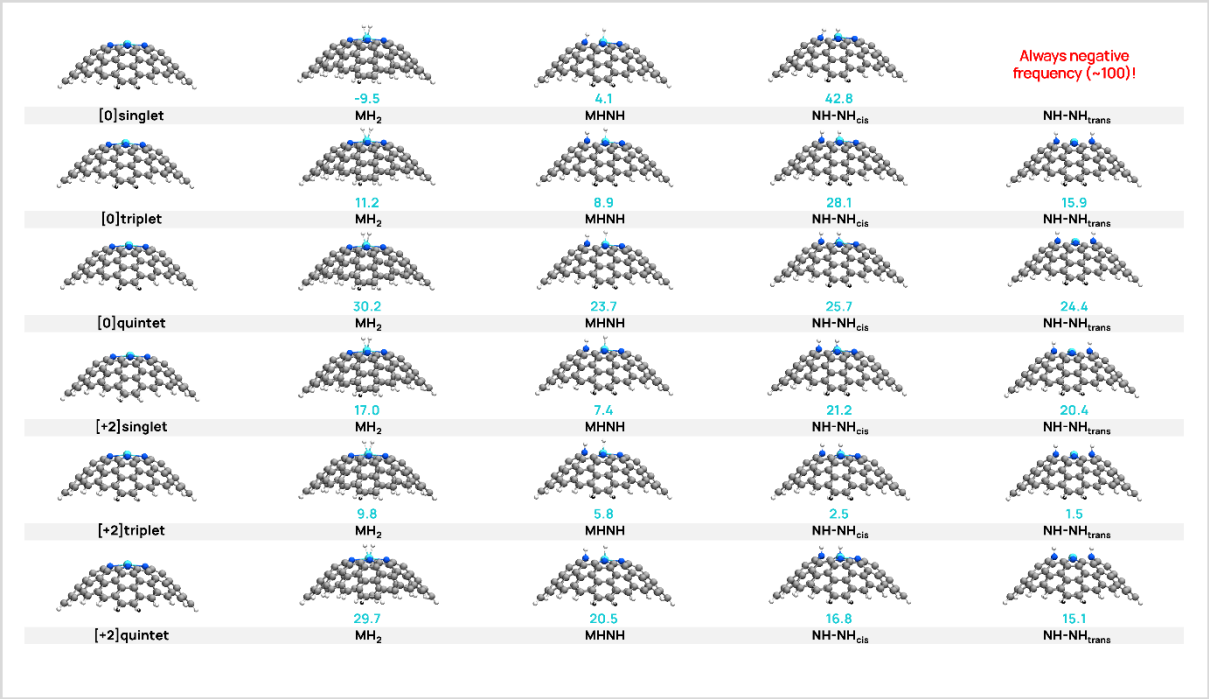


***Figure S8.*** *Optimized structures of Pyrr Ru complexes before and after $H_2$ addition, with corresponding ΔG values for the hydrogenation reaction (kcal·mol⁻¹).*

# Metal moving out of the plane

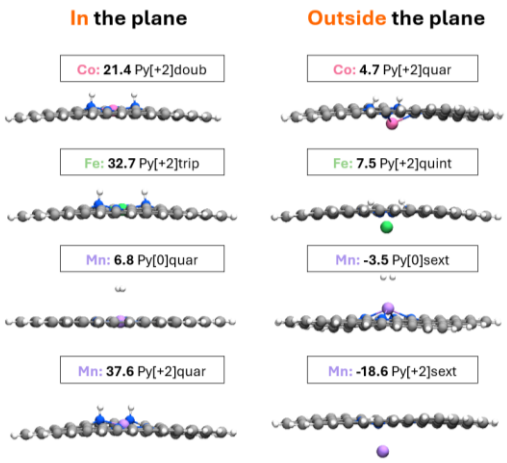


***Figure S9.*** *Metal in the plane and out of the plane intermediates for [+2]Py Co, [+2]Py Fe, [0]Py Co, and [+2]Py Mn systems.*

Other intermediates can be found for the systems where the metal moves out of the plane during hydrogenation, but exhibit systematically much higher ΔG.

# Triple-ζ versus double- ζ basis sets

The Gibbs free energy changes for the addition of H2 to three different systems have been computed with def2SVP and def2TZVP to evaluate the basis-set dependence (Figure S10). These calculations show significant energy differences of up to 10 kcal/mol. Nevertheless, the overall trend is the same: the Ru MH2 in Py is exergonic, the Co NHNHtrans in Pyrr is highly exergonic, and the same metal in a Py configuration is highly endergonic. This result, together with the high computational cost of performing energy refinements with def2TZVP for all calculated systems, led us to use def2SVP.

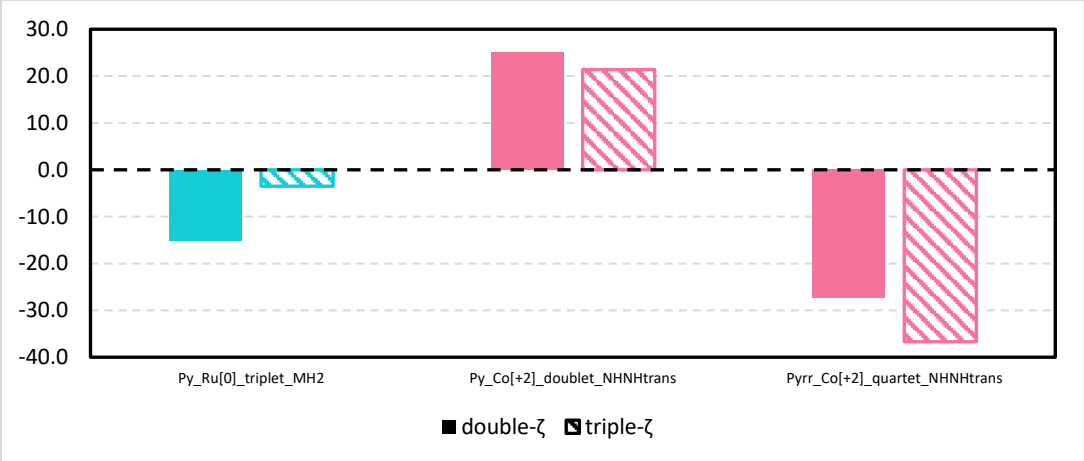


***Figure S10.*** *Free energy changes (ΔG, kcal mol$^{-1}$) for $H_2$ addition for a subset of systems calculated with a double-zeta (full bars) or a triple-zeta (dashed bars) basis set. Blue bars represent Ru systems and pink bars represent Co systems.*

# Hydrogenation without metals

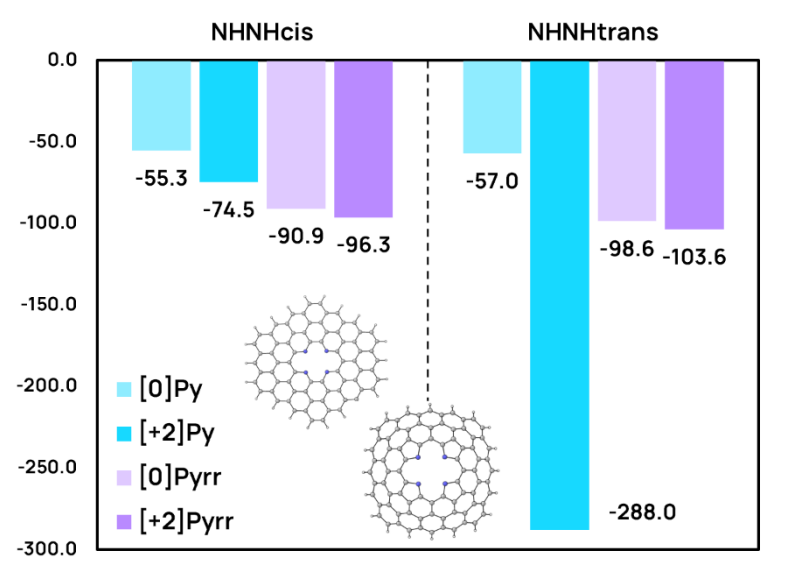


***Figure S11.*** *Gibbs free energies of $H_2$ addition for intermediates $NHNH_{cis}$ and $NHNH_{trans}$ in [0]Py, [+2]Py, [0]Pyrr, [+2]Pyrr systems (blue bars for Py systems, purple bars for Pyrr systems, lighter color bars for [0] systems, and darker color bars for [+2] systems).*

# NEDA Analysis

Through NEDA analysis, we explored the nature of metal-support interactions, focusing on the electrical (electrostatic (ES), polarization (POL)), charge transfer (CT), and exchange (X) components of the interaction energy between the metal atom and the support of the non-hydrogenated catalyst (Figure S13). Since the 3rd-row metals display similar results, they are discussed indistinctly.

Across [+2]Py, [0]Pyrr, and [+2]Pyrr models, systems containing Ru consistently exhibit a higher CT component than those with 1$^{st}$-row metals, while they have a lower electronic component, primarily arising from polarization (POL). A special case is [0]Py, in which the CT component is much higher than other models for the 1$^{st}$-row metals, even larger than for Ru. The least negatively charged nitrogen atoms and more neutral metal atoms of Ru systems are directly linked to higher CT and lower polarization components. Moreover, the exchange (X) component of the interaction energy is much more favorable than for the 1$^{st}$-row metal, indicating a stronger delocalization effect and covalent interactions. This reveals an enhanced electronic coupling between the metal and support, facilitating a flexible electron redistribution. Therefore, the Ru atom, akin to the homolytic cleavage in homogeneous catalysts, effectively uses its empty d-orbitals to accept electrons from the $H_2$ bonding orbital while back-donating electrons into the antibonding one to cleave the $H_2$ molecule. Conversely, the MHNH heterolytic cleavage, depending heavily on the nitrogen orbital accessibility, is less favorable on Ru systems. Moreover, the hydrogenation with the Ru metal atom is optimal in neutral systems, where the CT component predominantly influences the interaction energy.

In contrast, 1$^{st}$-row metal systems rely heavily on ionic interactions driven by their dominant electronic component. The lower CT results in the nitrogen orbitals of 1$^{st}$-row metal systems being more accessible, leading to more negative charges on these atoms, which increases their attraction to positively charged hydrogens and promotes an NHNH pathway. The higher polarization, ionic interaction, and lower CT are also the reasons for their enhanced reactivity on dicationic systems.

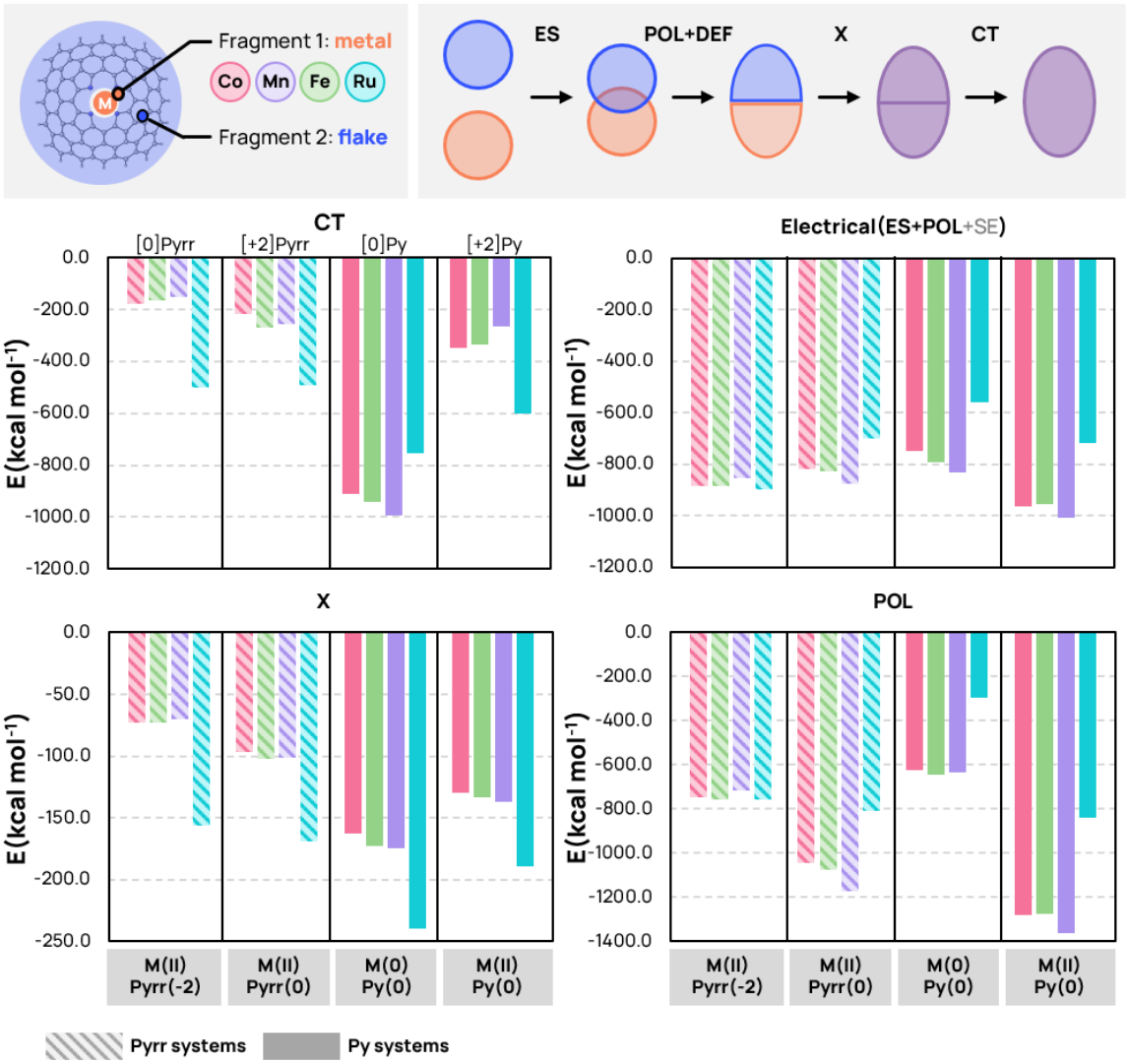


***Figure S12.*** *Natural energy decomposition analysis of metal-graphene fragment interactions (CT, Electrical, XC, POL) in Py and Pyrr models across for Co (pink bars), Mn (purple bars), Fe (greenn bars), Ru (blue bars) dicationic [+2] or neutral [0] systems.*

# Hydrogens natural charge

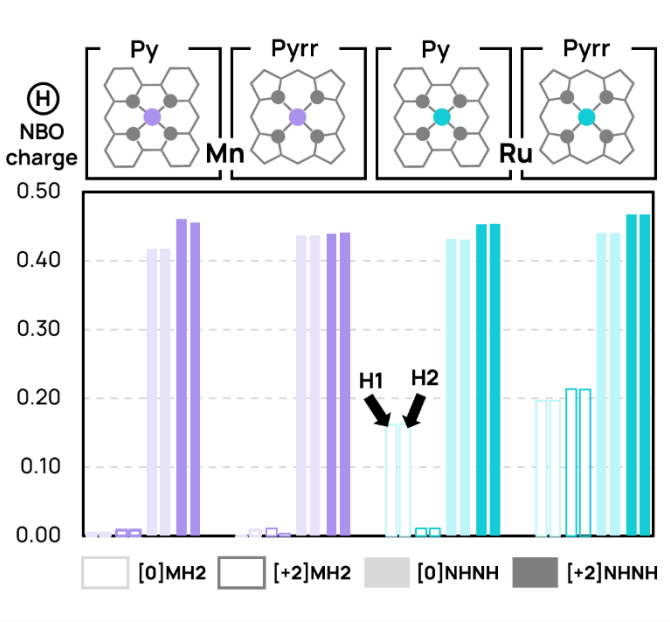


***Figure S13.*** *Natural charge of the two hydrogens (H1, H2) for Mn (purple bars) and Ru (blue bars) Pyrr and Py systems. Full bars indicate NHNH reactivity, while the others indicate MH2 reactivity. Faded colors indicate [0] systems, and darker colors represent [+2] systems.*

# Surface (M, Ns, Cs) natural charge change upon hydrogenation

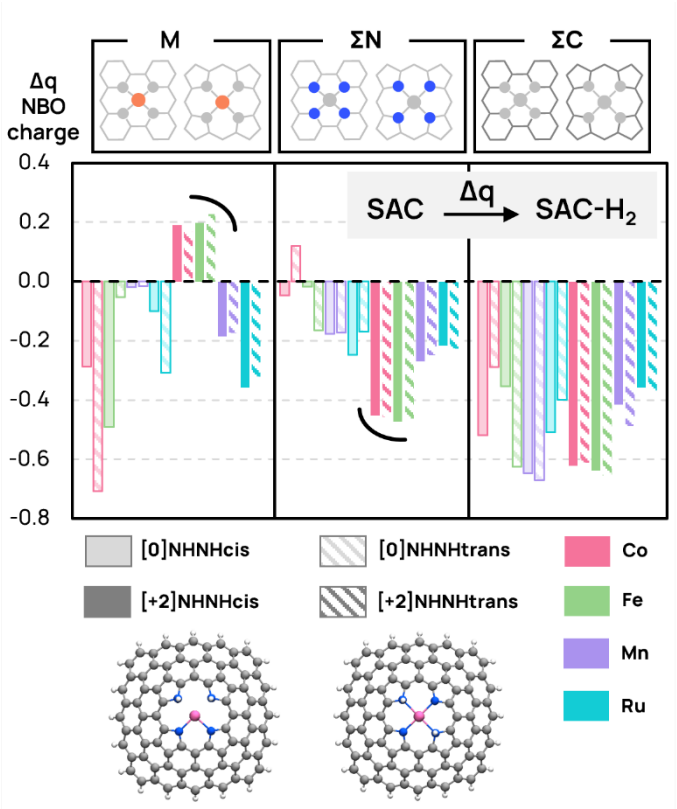


***Figure S14.*** *Change in natural charge of the metals ("M": Co, Fe, Mn, Ru), the four nitrogens (ΣN), and the carbons of the surface (ΣC) upon hydrogenation, on Pyrr systems NHNH reactivity. Full bars indicate $NHNH_{cis}$ reactivity while dashed bars represent $NHNH_{trans}$ reactivity. Faded colors represent [0] systems and dark colors [+2] systems.*

# Natural metal charge

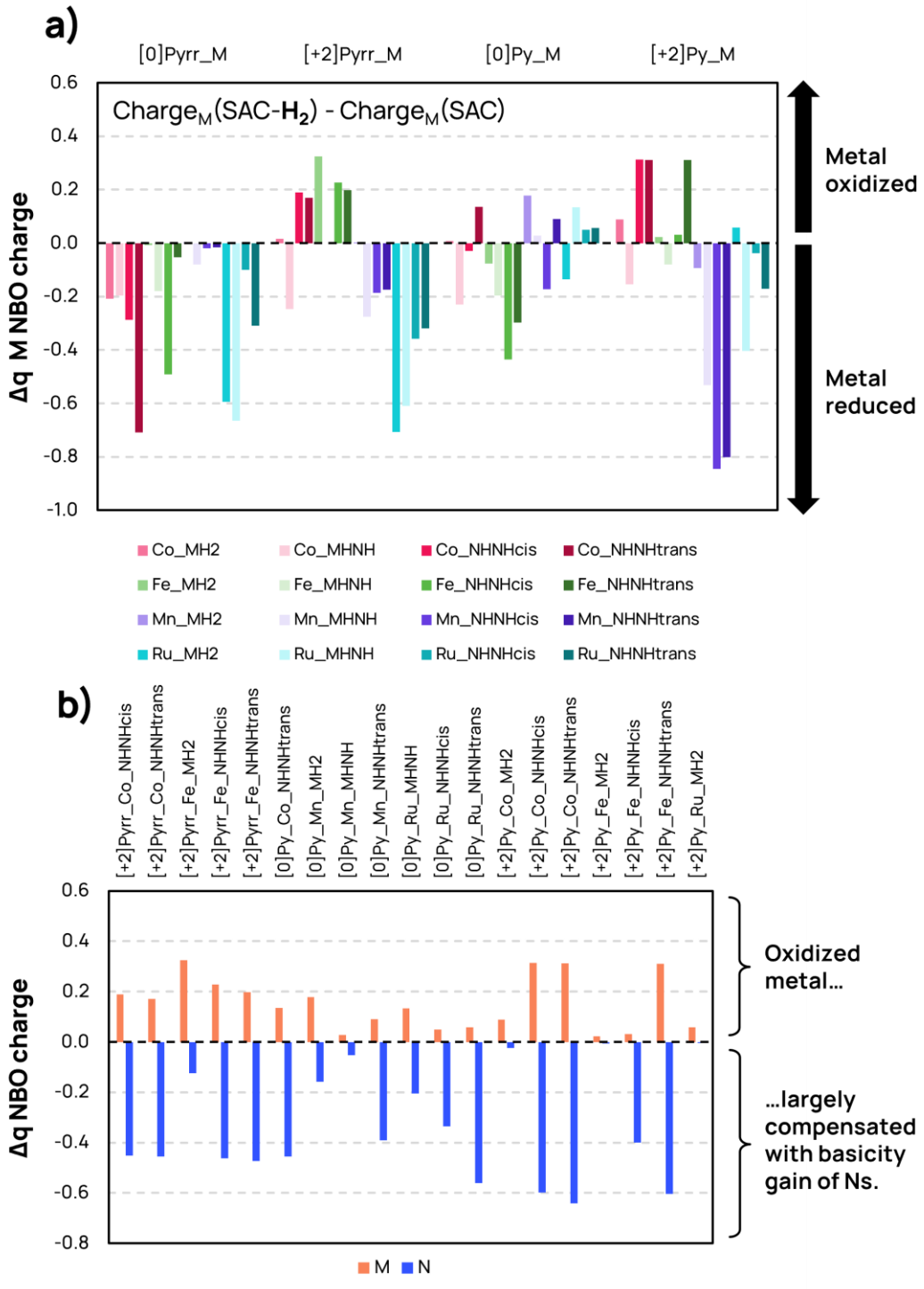


***Figure S15.*** *a) Change in natural charge of the metals ("M": Co, Fe, Mn, Ru) upon hydrogenation across all systems (Py, Pyrr models; MH2, MHNNH, NHNHcis, NHNHtrans intermediates), b) Corresponding change in natural charge on the metal (M) and nitrogens (N) atoms in systems with an oxidized metal, highlighting nitrogens as major electron acceptors.*

# Pristine structure and spin state influence

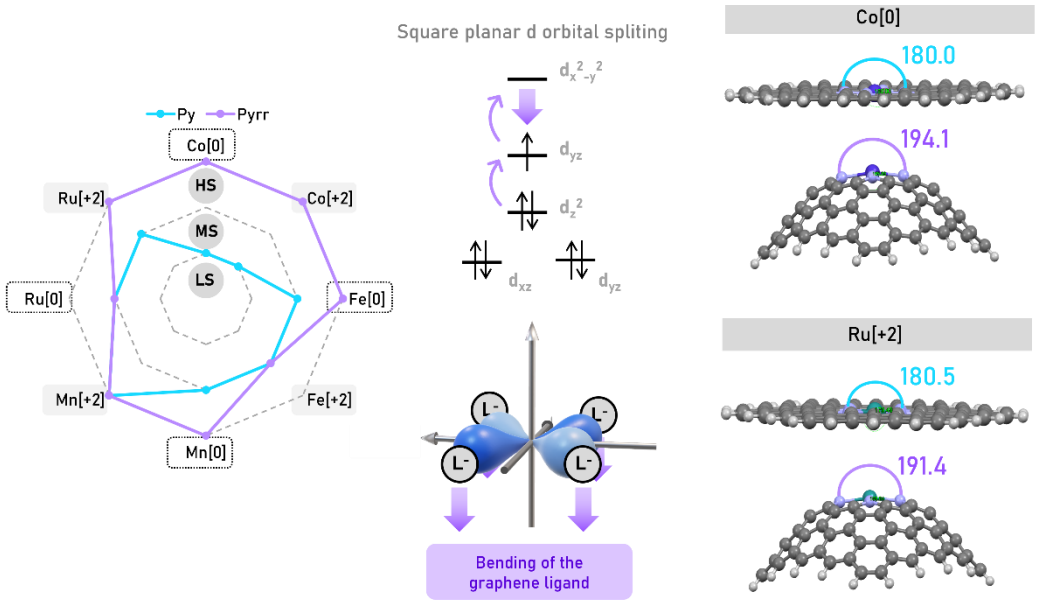


***Figure S16.*** *Left: spider chart of the spin state (LS, MS, HS) of the pristine SAC for Py systems in blue and Pyrr systems in purple. Middle: Schematic illustrating the influence of graphene curvature, which minimizes unfavorable interactions and lowers the dx2-y2 orbital, thereby favoring the HS configuration. Right: Surface angles for Co[0] and Ru[+2] Py and Pyrr systems.*

Comparing the different spin states for each model and metal for the pristine catalyst, we can notice a clear trend: The Pyrr model favors high spin, while the Py model favors a medium one. Given the nature of the flake (pyridinic or pyrrolic) being weak field ligands, and since three of the selected metals (Mn(II), Fe(II), Co(II)) also considered weak field, the high-spin nature of the ground state for most of these systems is not surprising. However, the Py model favors HS only for Mn[+2], while the Pyrr model favors it for all metals and charges, except for Fe[+2] and Ru[0].

This difference in pristine spin state can be understood from the structural differences between the two models, where the curvature in Pyrr allows the $d_{x2-y2}$ orbital to lower in energy, favoring single occupation of the d orbitals.

# Pristine to hydrogenated species: spin crossover

| Model-charge | Metal | Pristine spin state | Lowest intermediate spin state | |
|---|---|---|---|---|
| Py[0] | Fe | HS (quintet) | MS (triplet) | − |
| Py[0] | Mn | HS (sextet) | MS (quartet) | − |
| Py[0] | Ru | LS (singlet) | MS (triplet) | + |
| Pyrr[0] | Ru | LS (singlet) | MS (triplet) | + |
| Pyrr[+2] | Fe | HS (quintet) | MS (triplet) | − |
| Pyrr[+2] | Ru | MS (triplet) | HS (quintet) | + |

***Figure S17.*** *Table of systems that undergo spin crossover upon hydrogenation, including their model (Py, Pyrr), charge ([0], [+2]), metal (Fe, Mn, Ru), and spin state, as well as the lowest intermediate. The plus or minus signs indicate if the spin multiplicity of the system is lower (-) or higher (+) upon hydrogenation.*

When comparing the spin states of the most stable hydrogenated species with those of the pristine systems for each metal, we find that out of 16 cases, 6 exhibit spin crossovers. This phenomenon is more present for Py[0], where Mn, Fe, and Ru change spin state upon hydrogenation. It is also the case for the Ru systems, where 3 out of 4 systems show a spin state increase from the pristine to the hydrogenated species (singlet → triplet for Py[0], Pyrr[0], and triplet → quintet for [+2]Pyrr). However, for the two Fe systems (Py[0], Pyrr[+2]), the spin is lowered upon hydrogenation (quintet → triplet). Only the Co systems do not experience any change in spin state.